

Supporting Information

Revisiting the Gauche Oxygen Effect in $-\text{[O-CH}_2\text{-CHRO]-}$ ($\text{R}=\text{H/CH}_3$): Experimental Reassessment and Origin of Conformational Stability

Ken Tasaki[†]

Palos Verdes Research Institute, Redondo Beach, CA 90277

The reference number refers to the number under Reference in the manuscript unless described in the footnote.

1. Selection of Model Chemistry

Bally et al. have performed extensive computation of NMR ^1H - ^1H coupling constants of a variety of compounds using the gauge-including atomic orbitals (GIAO) method.^{S1} They presented two findings: 1) the two-step spin-spin coupling constant calculations (MIXED) significantly improves the root mean square deviation (RMSDE) of the calculated results and the experimental data; 2) the RMSDE of the results obtained using B3LYP/6-31(d,p)//B3LYP/6-31(d), was comparable to that obtained using B3LYP/cc-pVTZ//B3LYP/6-31G(d). This is significant because the CPU time of the latter calculations is up to four times that of the former calculations for a given molecule. Because their results include both geminal and vicinal coupling constants, obscuring the accuracy of the vicinal coupling constants separately, we attempted to find a reasonable model chemistry to describe the vicinal coupling constants for relevant model compounds: $\text{CH}_3\text{CH}_2\text{X}$ ($\text{X}=\text{H}, \text{CH}_3, \text{OH}, \text{F}, \text{CN}, \text{Cl}, \text{Br}$), and 1,2-propanediol

^{S1} Bally T, Rablen PR. Quantum-Chemical Simulation of ^1H NMR Spectra. 2. Comparison of DFT-Based Procedures for Computing Proton-Proton Coupling Constants in Organic Molecules. *J. Org. Chem.* **2011** Jun 17;76(12):4818-30.

(1,2-PD), and *cis*-2,6-dimethyl-1,4-dioxane (*cis*-DMDO), an analogous compound to 1,2-DMP, as shown in Figure 3a. The ¹H-¹H vicinal coupling constants for the CH₃-CH₂ bonds of the first group of model compounds can be expressed as an AX spin system averaged over the individual coupling constants owing to the symmetrical CH₃ rotation, yielding one experimental coupling constant measured between two peaks: one assigned to the CH₃ group and the other to the CH₂ group. In the case of ethane, ¹³C labeling was used to break its spin symmetry. Hence, a direct comparison between the calculated and experimental results is possible. For 1,2-PD, there are two known stable conformations: *g*⁺ around the CH₂-CH bond with a dihedral angle of ~60° and *g*⁻ with a dihedral angle of ~-60°, as shown in Figure 3b and 3c, respectively

These conformations are stabilized by the hydrogen bond between one oxygen atom and the hydrogen attached to another oxygen across the C-C bond, with *g*⁺ being more stable than *g*⁻.^{S2}

The coupling constant for the CH₂-CH bond of 1,2-PD can be calculated using the following equation:

$${}^3J_{CH_2-CH} = \left\{ (1/2) ({}^3J_{G_{H_1-H_2}}^{g^+} + {}^3J_{G_{H_1-H_3}}^{g^+}) \times e^{-\frac{\Delta E}{RT}} + (1/2) ({}^3J_{G_{H_1-H_2}}^{g^-} + {}^3J_{T_{H_1-H_2}}^{g^-}) \right\} / (e^{-\frac{\Delta E}{RT}} + 1) \quad (S1)$$

where ${}^3J_{G_{H_i-H_j}}^{g^\pm}$ and ${}^3J_{T_{H_i-H_j}}^{g^-}$ are the gauche and trans coupling constants across the hydrogen atoms *i* and *j* of the C-C bond of 1,2-PD, respectively, with the subscripts for the hydrogens shown in Figure 3b and c, and ΔE is the conformational energy difference between the *g*⁺ and *g*⁻ conformers.

The coupling constant averaged over various conformations may be calculated by the following equation:

^{S2} Caminati, W. Conformation and Hydrogen Bond in 1,2-Propanediol. *Journal of Molecular Spectroscopy*, **1981**, 86 (1), 193-201.

$${}^3J_{AB/AB} = \sum_i^n \left(\sum_j^l \frac{{}^3J_j}{l} \right) f_i^{CC/CO} \quad (\text{S2})$$

where 3J_j refers to the individual coupling constant for a given pair, j , of protons across the C-C bond, l is the number of relevant proton pairs for a given conformer i , and n is the number of conformers. f_i represents the Boltzmann fraction of conformer i , expressed as follows:

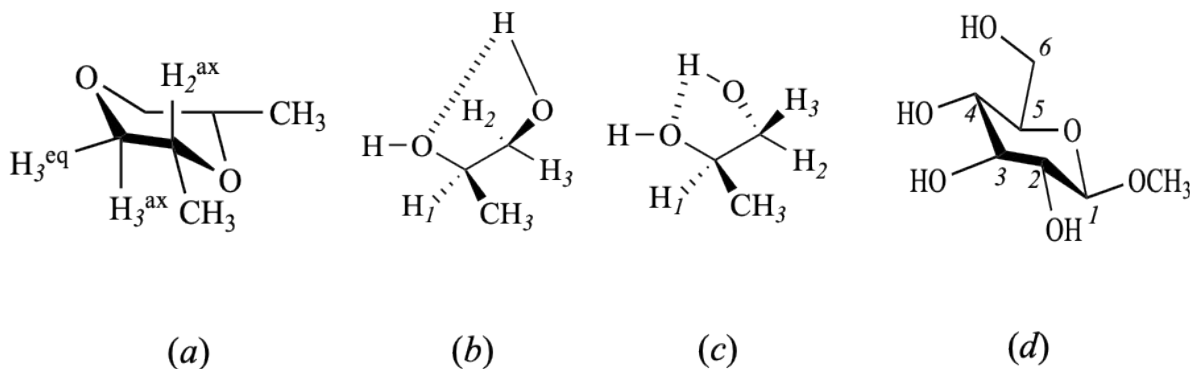
$$f_i^{CC/CO} = \frac{\exp\left(-\frac{\Delta E_i}{RT}\right)}{\sum_i \exp\left(-\frac{\Delta E_i}{RT}\right)} \quad (\text{S3})$$

We chose M06-2X/6-31+(2d,p)/M06-2X/6-31+G(2d,p), referred to as M06-2X in this study, as the model chemistry for calculating the NMR vicinal coupling constants and conformational energies, unless otherwise mentioned. Truhlar and coworkers developed improved exchange-correlation functionals, including the M05 and M06 series of functionals.³ In particular, the M06-2X functional is known to describe dispersion energy better than many other functionals, including the B3LYP.⁵³ Dispersion energy has been recognized to play an important role in calculating conformational energies of 1,2-disubstituted ethanes such as 1,2-DME.⁸

Table S1 summarizes the comparisons of calculations by the two model chemistries, B3LYP/6-31+G(2d,p)//B3LYP/6-31+G(2d,p), referred to as B3LYP, and M06-2X, against the experimental data of CH₃CH₂X (X=H, CH₃, OH, F, CN, Cl, Br), and 1,2-propanediol (1,2-PD), and *cis*-2,6-dimethyl-1,4-dioxane (*cis*-DMDO), the last two of which are analogous compounds to 1,2-DMP. Figure S1 illustrates some of the model compounds against which the model

⁵³ Y. Zhao, Y.; D.G., Truhlar. The M06 suite of density functionals for main group thermochemistry, thermochemical kinetics, noncovalent interactions, excited states, and transition elements: two new functionals and systematic testing of four M06-class functionals and 12 other functionals. *Theor Chem Account* **2008**, *120*, 215–241.

chemistries were tested. B3LYP reproduces the coupling constants reasonably well, except for 1,2-PD, which may be the most relevant model compound for 1,2-DME and 1,2-DMP among the model compounds tested here. In contrast, M06-2X yields excellent agreement with the experimental data, though this could be fortuitous, given the modest basis set. The normalized root mean square deviation of the M06-2X results is 0.09, compared to 0.15 for B3LYP. Though the number of compounds tested may not be sufficient to be statistically significant, M06-2X was chosen as a reasonable model chemistry specifically for 1,2-DME and 1,2-DMP. For the calculations of the $^{13}\text{C}-^1\text{H}$ Vicinal Coupling Constants ($^3J_{CH}$), we tested against those for methyl β -D-glucopyranoside (MGP), as shown in Figure S1d.²⁸ Table S2 lists the calculations performed



using M06-2X and B3LYP.

Figure S1. (a) *cis*-2,6-dimethyl-1,4-dioxane; (b) g^+ and (c) g^- around the C-C bond of 1,2-PD; (d) methyl β -D-glucopyranoside. The atoms are numbered in italics.

Table S1. ^1H - ^1H NMR Vicinal Coupling Constants of Tested Compounds Calculated by Two DFT Methods

	1,2-PD ^a	CH ₃ CH ₂ X X					<i>cis</i> -DMDO ^b	CH ₃ CH ₂ CH ₃	CH ₃ CH ₃	
		Br	Cl	CN	F	OH	$^3J_{H_2^{ax}-H_3^{eq}}$	$^3J_{H_2^{ax}-H_3^{ax}}$		
M06-2X ^c	4.03 ^e	7.49	7.49	7.37	7.19	7.18	2.4	9.2	6.96	7.70
B3LYP ^d	5.05 ^f	7.96	7.60	7.87	7.08	7.08	2.9	9.6	7.43	8.07
Exp.	4.00 ^g	7.35 ^h	7.26 ^h	7.26 ^h	7.00 ⁱ	7.00 ⁱ	2.5 ^j	10.3 ^j	7.26 ⁱ	8.02 ⁱ

^a1,2-propanediol.

^b*cis*-2,6-dimethyl-1,4-dioxane. The ^1H - ^1H pairs of coupling constants, $^3J_{H_2^{ax}-H_3^{eq}}$ and $^3J_{H_2^{ax}-H_3^{ax}}$, are shown in Figure S1a.

^cI. Ronen, A. G. Webb, ^1H NMR Spectroscopy of Strongly J-Coupled Alcohols Acquired at 50 mT (2 MHz) using a Carr–Purcell–Meiboom–Gill Echo Technique. *Pure Appl. Chem.* **2023**, *95* (10), 1067–1074. <https://doi.org/10.1515/pac-2023-0102>.

^dH. Günther, H. NMR Spectroscopy: Basic Principles, Concepts, and Applications in Chemistry. 2nd edition (English translation), John Wiley & Sons, 1995.

^eT. Bally, T.; P.R. Rablen, Quantum-Chemical Simulation of ^1H NMR Spectra. 2. Comparison of DFT-Based Procedures for Computing Proton-Proton Coupling Constants in Organic Molecules. *J. Org. Chem.* 2011, **76** (12), 4818-30. <https://doi.org/10.1021/jo200513q>.

^fY. Sasanuma, Solvent Effect on the Conformation of 1,2-Dimethoxypropane. *J. Phys. Chem.* 1994, **98** (51), 13486–88. <https://doi.org/10.1021/j100102a010>.

^cM06-2X/6-31+G(2d,p)//M06-2X/6-31+G(2d,p).

^dB3LYP/6-31+G(2d,p)//B3LYP/6-31+G(2d,p).

^eThe conformational energy of g^+ with respect to t around the C-C bond was calculated using M06-2X.

^fThe conformational energy of g^+ with respect to t around the C-C bond was calculated using B3LYP.

^gRef. S4; ^h Ref. S5; ⁱRef. S6; ^jRef.S7.

Table S2. ¹³C-¹H NMR Vicinal Coupling Constants of Methyl β-D-Glucopyranoside Calculated by Two DFT Methods^a

	³ J _{C₄-H₂}	³ J _{C₄-H_{6R}}	³ J _{C₄-H_{6R}}	³ J _{C₅-H₃}	³ J _{C₆-H₄}
M06-2X	1.3	0.6	2.1	1.4	3.8
B3LYP	1.5	0.2	2.2	1.6	4.0
Exp. ^b	1.1	1.0	2.4	1.1	3.6

^aSee Figure S1d.; ^b Ref. 32.

2. Geometry Optimization

Geometry optimizations were conducted using the ULTRAFINE integration grid and TIGHT convergence criteria. Initial structures for each conformer were generated via relaxed torsional scans in which the relevant dihedral angle was fixed while all other geometrical parameters were optimized. The resulting local minima were subsequently fully optimized without constraints. Harmonic frequency calculations were performed for all optimized structures to confirm that they correspond to true minima with no imaginary frequencies. All calculations were carried out in the gas phase.

3. NMR Coupling Constants

All previous studies adopted the assumption that ${}^3J_T = {}^3J_T'$ and ${}^3J_G = {}^3J_G' = {}^3J_G'' = {}^3J_G'''$ for the conformational study for 1,2-DME and 1,2-DMP.¹⁰⁻¹² This assumption reduced the unknown parameters from six to two: 3J_T and 3J_G . The assumption allowed determination of the conformational energy around the C-C bond of 1,2-DME by least-squares fitting to the NMR data.¹⁰ For 1,2-DMP, the values of 3J_T and 3J_G were adopted from those of the analogous compound, cis-2,6-dimethyl-1,4-dioxane (cis-DMDO), while retaining the same assumption above without accounting for differences in the C-C dihedral angles between cis-DMDO and the 1,2-DMP conformations.⁴

The Karplus equations for the ${}^1\text{H}$ - ${}^1\text{H}$ and ${}^{13}\text{C}$ - ${}^1\text{H}$ coupling constants for 1,2-DME and 1,2-DMP are given as follows:

$${}^3J_{AB(AC)/AB'(BC)}(\phi_{CC/CO}) = a_j^i \cos^2 \phi_{CC} + b_j^i \cos \phi_{CC} + c_j^i \quad (\text{S4})$$

where a_j^i , b_j^i and c_j^i represent the coefficients for the bond j (= the C-C or C-O bond) of the molecule i (=1,2-DME or 1,2-DMP). $\phi_{CC/CO}$ refers to the dihedral angles around the C-C or C-O bond of 1,2-DME and 1,2-DMP, respectively.

Table S3. The Coefficients for Karplus Equations for the C–C/C–O bonds of 1,2-DME and the C–C bond of 1,2-DMP (Hz).

		a_j^i	b_j^i	c_j^i
$i = 1,2\text{-DME}$	$j = \text{CC}$	10.21	-0.70	0.56
	$j = \text{CO}$	10.51	-0.42	0.34
$i = 1,2\text{-DMP}$	$j = \text{CC}$	8.63	-0.48	0.13

For example, 18-crown-6, an analogous compound to 1,2-DME, has been reported to have a $^1\text{H}\text{--}^1\text{H}$ vicinal coupling constant across the C–C bond of 5.4–5.5 Hz, which is an average of the trans and gauche around the C–C bond, given the flexible bond rotation.³¹ We optimized the geometry of 18-crown-6 to determine the dihedral angles of the protons across the C–C bonds of 18-crown-6. The average dihedral angles for the trans and gauche conformers were 170.2° and 54.12°, respectively. The substitution of these angles into eq 6 yields an average coupling constant of 5.5 Hz, depicted by the blue circles in Figure 3a, which are in good agreement with the experimental data.³¹ For $^3J_{\text{CH}}$, the experimental data of b-D-glucopyranoside (MGP) are included in Figure 3b. The geometry of MGP was also optimized using M06-2X. The Karplus curve shows a fair agreement with the experimental data.³² For 1,2-DMP, the experimental $^1\text{H}\text{--}^1\text{H}$ coupling constants of *cis*-2,6-dimethyl-1,4-dioxane (*cis*-DMDO) are also included in Figure 3c by the blue circles, after determining the dihedral angles (ϕ_{CC}) of the corresponding $^1\text{H}\text{--}^1\text{H}$ pairs using M06-2X. The experimental data are reasonably well reproduced by the Karplus curve.

4. Conformational Energies and Total Electronic Energies of 1,2-DME and 1,2-DMP

Table S4 summarizes the conformational energies of $tg^\pm t$ or g^\pm relative to ttt or t for 1,2-DME, 1,2-DMP, 1,2-DFE, and *n*-butane, respectively, at various theoretical levels, based on the electronic energies. Table S5 includes the electronic energies of each conformation in a.u. Tsuzuki et al. used the 6-311++G* basis set for their MP4 calculations of 1,2-DME on the geometry optimized by HF/6-311+G* calculations.⁵ In contrast, Jaffe et al. utilized the D95+(2d,f,p) basis set for MP2 calculations of 1,2-DME on the geometry optimized by MP2 calculations.⁶ The D95+(2d,f,p) basis set is considered outdated. On the other hand, the cc-pVTZ basis set has been developed for correlated methods such as the MP2 method and is considered to be more reliable than the D95 basis sets or 6-311++G* basis set for higher-level methods.³¹ The inclusion of electron correlation in the calculation of the conformational energies of 1,2-DME has been emphasized.⁵ The M06-2X calculations with the 2*d* functions on the heavy atoms yielded an energy difference between the two conformers close to that of the MP4 calculations at a fraction of the CPU time required for the latter.

Table S4. The Conformational Energies for the C-C bond of XCH₂CH(R)X (X=CH₃O, F, CH₃; R=H, CH₃) (kcal mol⁻¹)^a

Model Chemistry	ΔE_{conf} , kcal mol ⁻¹					
	1,2-DME		1,2-DMP		1,2-DFE	<i>n</i> -butane
X	CH ₃ O		CH ₃ O		F	CH ₃
R	H		CH ₃		–	–
	<i>tg</i> [±] <i>t</i>	<i>g</i> [∓] <i>g</i> [±] <i>t</i>	<i>tg</i> ⁻ <i>t</i>	<i>tg</i> ⁺ <i>t</i>	<i>g</i> [±]	<i>g</i> [±]
M06-2X/6-31+G(2d,p) //M06-2X/6-31+G(d,p)	0.36	0.38	1.03	1.19	-0.78	0.56
MP2/cc-pVTZ //MP2/cc-pVTZ	0.22	0.18	0.98	1.18	-0.76	0.56
MP4/cc-pVTZ //MP2/cc-pVTZ	0.26	0.12	0.94	1.19	-0.66	0.57

Table S5. Electronic Energies for Conformers around the C-C bond of XCH₂CH(R)X (X=O, F, CH₃; R=H, CH₃) (a.u.)^a

Model Chemistry	E_{elec} , kcal mol ⁻¹									
	1,2-DME			1,2-DMP			1,2-DFE		<i>n</i> -butane	
	CH ₃ O			CH ₃ O			F		CH ₃	
	H			CH ₃			–		–	
X										
R										
	<i>ttt</i>	<i>tg[±]t</i>	<i>g[∓]g[±]t</i>	<i>ttt</i>	<i>tg⁻t</i>	<i>tg⁺t</i>	<i>t</i>	<i>g[±]</i>	<i>t</i>	<i>g[±]</i>
M06-2X/6-31+G(2d,p)	-277.8785	-308.7403	-308.7402	-347.8615	-347.8600	-347.8596	-158.0730	-278.2025	-158.3746	-158.3737
//M06-2X/6-31+G(d,p)										
MP2/cc-pVTZ	-308.2704	-308.2701	-308.2702	-347.4981	-347.4965	-347.4965	-277.5892	-277.8785	-158.0739	-158.0730
//MP2/cc-pVTZ										
MP4/cc-pVTZ	-308.3703	-308.3699	-308.3701	-347.6156	-347.6142	-347.6142	-277.9321	-277.9332	-158.1535	-158.1526
//MP2/cc-pVTZ										

^aThe energies are expressed in a.u.

5. NEDA Components and SOPE Results for Each Conformation

Table S6. NEDA Energy Terms for Various Conformations of XCH₂-CHRX (X=CH₃O/F, R=H/CH₃) (kcal mol⁻¹).

	1,2-DME		1,2-DMP			1,2-DFE		<i>n</i> -butane	
	<i>ttt</i>	<i>tg</i> [±] <i>t</i>	<i>ttt</i>	<i>tg</i> ⁻ <i>t</i>	<i>tg</i> ⁺ <i>t</i>	<i>t</i>	<i>g</i> [±]	<i>t</i>	<i>g</i> [±]
ΔE_{CT}	-475.28	-485.59	-470.01	-475.80	-472.34	-461.53	-474.84	-460.61	-455.31
ΔE_{EL}	-105.73	-106.97	-113.24	-113.60	-113.56	-97.64	-100.1	-110.21	-111.36
ΔE_{CORE}	469.67	481.21	473.60	481.40	477.51	452.20	467.36	461.267	457.73
ΔE_{XC}	-41.85	-42.41	-46.42	-45.97	-47.15	-36.13	-37.21	-45.35	-46.38
ΔE_{DEF}	461.5	474.10	472.51	478.61	479.13	429.90	445.59	459.95	460.89
ΔE_{SE}	-50.01	-49.82	-47.51	-47.95	-45.54	-58.28	-58.98	-46.668	-43.19
ΔE_b	-111.34	-111.05	-109.65	-109.20	-108.39	-106.98	-107.58	-109.55	-108.94
E_{steric}^{NSA}	87.34	87.89	206.26	206.28	207.62	87.06	88.25	80.57	83.3

Table S7. SOPE for Pairwise Orbital Interactions for Conformations of XCH₂ - CH(R)X (X=CH₃, O, and F; R=H, CH₃) (kcal mol⁻¹).

$E^{(2)}$	1,2-DME		1,2-DMP			1,2-DFE		Butane	
	$t t t$	$t g^{\pm} t$	$t t t$	$t g^{+} t$	$t g^{-} t$	t	g^{\pm}	t	g^{\pm}
$\sigma_{C_1-H_3} \rightarrow \sigma_{C_2-H_5}^*$	2.78	0	–	–	–	2.33	0	3.37	0
$\sigma_{C_1-H_3} \rightarrow \sigma_{C_2-H_6}^*$			0	0	3.23	0	0		
$\sigma_{C_1-H_3} \rightarrow \sigma_{C_2-X_8}^*$	0	3.88	0	4.60	1.17	0	4.87	0	3.87
$\sigma_{C_1-H_4} \rightarrow \sigma_{C_2-H_6}^*$	2.78	0.0	3.16	0	0	2.33	0	3.37	0.0
$\sigma_{C_1-H_4} \rightarrow \sigma_{C_2-H_5}^*$	0	2.78	–	–	0	0	2.53	0	3.36
$\sigma_{C_1-H_4} \rightarrow \sigma_{C_2-X_8}^*$	0	1.62	0	1.12	4.31	0	1.65	0	0
$\sigma_{C_1-X_7} \rightarrow \sigma_{C_2-X_8}^*$	1.57	0.0	2.01	0	0	1.55	0	2.32	0
$\sigma_{C_1-X_7} \rightarrow \sigma_{C_2-H_6}^*$	0	1.00	0	1.34	0	0	0.76	0	1.62
$\sigma_{C_2-H_5} \rightarrow \sigma_{C_1-H_3}^*$	2.78	0.0	–	–	–	2.33	0	3.37	0.0
$\sigma_{C_2-H_5} \rightarrow \sigma_{C_1-H_4}^*$	0	2.78	–	–	–	0	2.53	0	0
$\sigma_{C_2-H_5} \rightarrow \sigma_{C_1-F_7}^*$	0	1.62	–	–	–	0	1.65	0	0
$\sigma_{C_2-H_6} \rightarrow \sigma_{C_1-X_7}^*$	0	3.88	0	4.94	1.16	0	4.87	0	3.87
$\sigma_{C_2-H_6} \rightarrow \sigma_{C_1-H_4}^*$	2.78	0	3.28	0.0	0	2.33	0	3.37	0
$\sigma_{C_2-H_6} \rightarrow \sigma_{C_1-H_3}^*$	0	0	0	0	3.16	0	0	0	0
$\sigma_{C_2-X_8} \rightarrow \sigma_{C_1-X_7}^*$	1.57	0	2.26	0	0	1.55	0	2.32	0
$\sigma_{C_2-X_8} \rightarrow \sigma_{C_1-H_3}^*$	0	1.00	0	1.39	0	0	0.76	0	1.62
$\sigma_{C_1-H_3} \rightarrow \sigma_{C_2-C_5}^*$	–	–	3.97	4.11	0	–	–	–	–
$\sigma_{C_2-C_5} \rightarrow \sigma_{C_1-H_3}^*$	–	–	1.88	0	0	–	–	–	–
$\sigma_{C_2-C_5} \rightarrow \sigma_{C_1-O_7}^*$	–	–	0	1.96	2.82	–	–	–	–